



Behavior of post-installed anchors tested by stepwise increasing cyclic crack protocols

Journal:	<i>ACI Structural and Materials Journals</i>
Manuscript ID	S-2015-342.R1
Journal Name:	ACI Structural Journal
Date Submitted by the Author:	n/a
Complete List of Authors:	Mahrenholtz, Christoph Eligehausen, Rolf; University of Stuttgart Hutchinson, Tara; University of California, San Diego Hoehler, Matthew; Hilti North America, Engineering Services
Keywords:	anchor, crack cycling, crack, earthquake, axial load, testing

1
2
3
4
5
6
7
8
9
10
11
12
13
14
15
16
17
18
19
20
21
22
23
24
25
26
27
28
29
30
31
32
33
34
35
36
37
38
39
40
41
42
43
44
45
46
47
48
49
50
51
52
53
54
55
56
57
58
59
60

1 **BEHAVIOR OF POST-INSTALLED ANCHORS TESTED BY** 2 **STEPWISE INCREASING CYCLIC CRACK PROTOCOLS**

3 Christoph Mahrenholtz, Rolf Eligehausen, Tara C. Hutchinson and Matthew S. Hoehler

4
5 **Christoph Mahrenholtz** is R&D Manager at Jordahl in Berlin, Germany. He received
6 his diploma from the University of Karlsruhe (KIT), Karlsruhe, Germany, and his PhD in
7 civil (structural) engineering from the University of Stuttgart, Germany. His research
8 interests include cast-in-place and post-installed anchors and reinforcing bars subjected to
9 seismic actions.

10 **Rolf Eligehausen**, FACI, is a Professor Emeritus at the Institute of Construction
11 Materials at University of Stuttgart, Stuttgart, Germany. He is a member of ACI Committees
12 349, Concrete Nuclear Structures, 355, Anchorage to Concrete, and Joint ACI-ASCE
13 Committee 408, Development and Splicing of Deformed Bars and is chairman of the fib Task
14 Group 2.9 “Fastenings to Concrete and masonry Structures”. His research interests include
15 anchorage to concrete as well as bond and detailing of reinforcement.

16 **Tara C. Hutchinson** is a Professor at the University of California, San Diego in the
17 Department of Structural Engineering. She received her MS from the University of Michigan,
18 Ann Arbor, MI, and her PhD from the University of California, Davis. Her research interests
19 include earthquake engineering, including the performance evaluation of soil-foundation
20 systems, concrete components, nonstructural systems and components, and development of
21 damage-monitoring strategies.

22 **Matthew S. Hoehler** is a Research Structural Engineer at the National Institute of
23 Standards and Technology in Gaithersburg, Maryland (formerly with Hilti Corporation). He
24 received his BS from Princeton University, his MS from the University of California,
25 Berkeley, and his PhD from the University of Stuttgart, Germany. His research interests

1 include experimental testing and analysis of the performance of materials, components, and
2 structures associated with structural collapse, natural disasters, or human-initiated events.

4 ABSTRACT

5 Opening and closing of cracks due to cyclic demands imposed on reinforced concrete
6 structures is one of the most demanding actions to which anchorages in concrete are
7 subjected. These actions can result in degraded load capacities or even failure of the
8 anchorage. To achieve reliable anchor performance in earthquakes, consideration of crack
9 movement behavior is essential during product qualification testing. Qualification tests on
10 post-installed concrete anchors according to the American Concrete Institute (ACI) standard
11 ACI 355 consider crack movement caused by repeated live loads only; requiring a large
12 number of small amplitude crack cycles. In contrast, recent research has shown that stepwise-
13 increasing cyclic crack protocols with a moderate number of cycles better represents the
14 conditions anticipated during earthquakes. This paper investigates the load-displacement
15 behavior of common post-installed anchors in stepwise-increasing crack movement tests that
16 were recently adopted in European approval guidelines for seismic qualification of post-
17 installed anchors.

18
19 **Keywords:** Anchor; crack cycling; crack; earthquake; axial load; testing

21 INTRODUCTION

22 During earthquakes, structures undergo reversed cyclic deformation, which may cause
23 opening and complete closing of cracks in reinforced concrete structures. If post-installed
24 concrete anchors are located in these cracks, which is likely since anchors tend to attract
25 cracks¹, the anchors can experience substantial displacement when they are loaded axially

1 and simultaneously subjected to crack cycling (Fig. 1). The characteristics of seismic crack
2 cycles (amplitude, frequency and number) differ from the crack movement tests in the
3 American Concrete Institute (ACI) standards ACI 355.2² and ACI 355.4³ to qualify
4 mechanical and adhesive anchor products for use in cracked concrete in non-seismic
5 applications according to ACI 318⁴. The non-seismic crack movement tests, which have a
6 relatively small maximum crack width of 0.3 mm (0.012 in.) and a relatively large number of
7 crack opening and closing cycles (1000), are intended to mimic the effects of live load or
8 thermal load variation over the service life (50 years) of the anchors (Fig. 2). This test is one
9 of the most demanding anchor qualification tests, despite the small crack width prescribed.
10 Qualification of post-installed anchors for seismic applications in the United States currently
11 requires only simulated seismic tension and shear load cycling tests in a non-moving (static)
12 crack width of 0.5 mm (0.020 in.). Historically, the European Technical Approval Guideline
13 (ETAG) for post-installed anchor qualification ETAG 001⁵ did not cover seismic use. This
14 limitation was a motivation for the research presented in this paper.

15 Early studies of anchor behavior in cycled cracks conducted by Rehm and Lehmann⁶
16 investigate expansion anchors installed in simply supported reinforced concrete members that
17 were cyclically loaded to open and close the cracks by bending. They found that
18 progressively increasing anchor displacement during crack cycling indicates imminent failure.
19 Later studies by Lotze and Faoro⁷ establish that 1000 crack cycles with a maximum crack
20 width of 0.3 mm (0.012 in.) is representative for a 50 year anchor service life. Their tests on
21 undercut anchors show that anchor displacement behavior also depends on the crack closing
22 width during crack cycling and that the anchor influences the crack width as it generates
23 splitting forces in the concrete member. Eligehausen and Asmus⁸ evaluate acceptable
24 displacements for anchors during crack cycling and propose a limit on displacements of
25 2 mm (0.08 in.) after 20 crack cycles and 3 mm (0.12 in.) after 1000 cycles with a maximum

1 crack width of 0.3 mm (0.012 in.). A sustained tension load on the anchor of 1.3 times the
2 allowable service load was prescribed during crack cycling. While the aforementioned studies
3 provide useful indications of anchor displacement capacity during crack cycling, all were for
4 non-seismic applications.

5 During seismic events, the number of crack cycles is far fewer than that experienced
6 during the service life of the anchor however the crack widths are larger. Such extreme,
7 transient events may cause reinforcing steel to experience large strains and crack widths may
8 increase significantly. Therefore, qualification of anchors according to the German Guideline
9 for Anchorages in Nuclear Power Plants⁹, which is intended to cover extreme events such as
10 earthquakes, includes cyclic crack tests in large cracks of up to 1.5 mm (0.06 in.) width. In
11 these procedures however, only 10 crack cycles of constant amplitude are imposed. The
12 minimum crack width during crack cycling is taken as 0.5 mm (0.02 in.) smaller than the
13 maximum crack width. These crack widths assume that the reinforcing steel in the concrete
14 has yielded. Hoehler and Eligehausen¹⁰ conducted simulated seismic crack tests with post-
15 installed and cast-in anchors with a targeted maximum crack width of 0.8 mm (0.03 in.) and
16 ten equal-amplitude cycles. The maximum crack width was based on analytical studies of
17 crack widths just outside of plastic hinges, assuming non-yielding reinforcement, in flexural
18 members designed according to Eurocode 2¹¹ and Eurocode 8¹² and cyclic damage
19 accumulation during earthquakes. During these tests, cracks were opened under load control
20 and forced closed by compressing the concrete test member with up to 15 % of the concrete
21 compressive strength to capture the effects of moment reversals in structural members during
22 earthquakes. The authors demonstrate experimentally that a compressive stress of 10 % to
23 15 % of the concrete compressive strength is sufficient to achieve crack closure and that their
24 protocol provides a conservative indication of seismic anchor performance outside of plastic
25 hinge zones of reinforced concrete members¹⁰. It is noted that neither the design provisions

1 nor qualification guidelines in the United States or Europe cover anchors installed in plastic
2 hinge zones. Hoehler and Elgehausen conclude that full closure of the crack cannot be
3 substituted by increasing the crack opening width to maintain a representative difference
4 between maximum and minimum values, e.g. crack cycling between 1.0 mm (0.04 in.) and
5 0.2 mm (0.008 in.) instead of 0.8 mm (0.03 in.) and 0.0 mm (0.0 in.), which would simplify
6 testing.

7 More recently, extensive numerical investigations of the deformation behavior of
8 reinforced concrete structures in high-seismic regions performed by Wood and Hutchinson
9 resulted in a proposal for an anchor crack cycling test protocol^{13,14}. In the present study, the
10 Wood and Hutchinson crack cycling protocol is adopted, together with an improved test setup,
11 to investigate seismic behavior of common post-installed anchors under representative and
12 precisely-controlled conditions. The present effort was part of an extensive research program
13 carried out at the *Institut für Werkstoffe im Bauwesen, Universität Stuttgart (IWB)*¹⁵ to help
14 develop the new European Technical Approval Guideline for seismic testing of concrete
15 anchor.

16 17 **RESEARCH SIGNIFICANCE**

18 This paper provides comprehensive data from simulated seismic crack cycling tests
19 conducted on concrete anchors for the first time using direct crack width control and
20 stepwise-increasing crack width protocols. The tested anchors were from various
21 manufacturers and cover the most common post-installed anchor types and critical failure
22 modes. Test results demonstrate the effect of the crack protocol on the displacement and load
23 capacity of the investigated anchors. Furthermore, these tests increase understanding of
24 anchor behavior in earthquake-relevant crack conditions – thus supporting the design of safer

1 anchors in seismic applications – and form the basis for the development of seismic crack
2 anchor qualification test procedures.

4 EXPERIMENTAL INVESTIGATION

5 Fourteen cyclic and monotonic test series were conducted, typically with three test
6 repeats per series, resulting in a total of 74 individual anchor tests. The primary goals of the
7 tests were to investigate the performance of common anchor types under axial load and
8 representative simulated seismic cycled cracks. These tests aimed to generate load-
9 displacement curves for governing anchor failure modes and to study the effectiveness of
10 using a stepwise-increasing crack cycling protocol to simulate the seismic behavior of
11 anchors.

13 Anchors and concrete

14 Eight medium-size (10 mm to 16 mm (3/8 in. to 5/8 in.) nominal diameter) anchor
15 products from various manufacturers were investigated, of which five were mechanical and
16 three were adhesive anchors (Table 1). One self-cutting undercut anchor (UA1), one screw
17 anchor (SA1), one sleeve-type and two bolt-type torque-controlled expansion anchors (EAs1
18 and EAb1, EAb2), two bonded anchors with epoxy-formulations (BA1, BA2) as well as one
19 bonded anchor with a methacrylate-formulation (BA3) (all bonded anchors with threaded rod
20 M12) were tested. The screw anchor was qualified according to ETAG 001⁴ for use in
21 uncracked and cracked concrete (non-seismic) and all other investigated anchor products
22 were qualified according to ACI 355 including seismic applications. Fig. 3 illustrates the
23 tested anchor types as well as the corresponding load transfer mechanisms after crack
24 opening.

1
2
3 1 The concrete test members were constructed of normal weight concrete with a nominal
4
5 2 concrete compressive strength of $f'_c = 20$ MPa (2900 psi). Reference tests were carried out in
6
7 3 1635 mm \times 1550 mm \times 260 mm (64 in. \times 61 in. \times 10 in.) wedge-split concrete slabs as
8
9
10 4 reported by Mahrenholtz¹⁶. Strain-split concrete slabs 700 mm \times 420 mm \times 270 mm (27.5 in.
11
12 5 \times 16.5 in. \times 10.5 in.) were used as the anchorage material for the cyclic crack tests (Fig. 4).
13
14 6 The strain-split specimens were designed to test single anchors where the crack width is
15
16
17 7 controlled with high precision. Four high-strength (yield strength ≥ 950 MPa (138 ksi)) tie
18
19 8 rods with bar diameter d_b equal to = 15 mm (0.59 in.) were cast lengthwise in the concrete
20
21 9 slab and protruded at both ends of the specimen. Two 2 mm (0.8 in.) thick metal sheets were
22
23 10 embedded in the concrete through the depth of the specimen on both sides of the calculated
24
25 11 crack location to aid crack formation (Fig. 4). Additionally, the tie rods were debonded from
26
27
28 12 the concrete on both sides of these crack inducers over a total length of 500 mm (20 in.) to
29
30 13 facilitate large crack widths while allowing the reinforcement to remain elastic. Pilot holes
31
32 14 10 mm (0.39 in.) in diameter were drilled at the center of the slab to help ensure that the
33
34 15 crack transects the anchor location after the slab is cracked. A hairline crack was generated
35
36 16 by hammering wedges into hardened metal sleeves placed in two prefabricated holes along
37
38 17 the crack plane. After a hairline crack appeared, the wedges were removed and the pilot hole
39
40 18 was re-drilled to the required diameter for the investigated anchor. The anchors were then
41
42 19 installed according to the manufacturers' published installation instructions. The installation
43
44 20 torque was reduced to 50 % of the installation value immediately prior to testing to account
45
46 21 for relaxation as specified in ACI 355.
47
48
49
50
51
52
53
54
55
56
57
58
59
60

23 **Crack protocol, target crack width and sustained anchor tension load**

24 The crack protocols utilized for these tests were developed using the results of
25 nonlinear finite element simulations of reinforced concrete buildings representative of typical

1 building stock in high-seismic regions of the world with mature building seismic design
2 codes¹⁵. The stepwise-increasing protocols were derived using Rainflow counting (an
3 algorithm to reduce an arbitrarily varying time series to a set of simple reversals) of building
4 member curvatures extracted from the nonlinear time-history analyses of seven buildings
5 ranging from 2- to 20-stories, which were subjected to 21 amplitude-scaled earthquake
6 ground motions. The cycle counting, after normalization, re-arranging with respect to their
7 amplitudes, and averaging, resulted in several crack cycling protocols that differed depending
8 on the level of statistical significance and processing method. For the present study, the
9 protocol involved 32 crack cycles with the crack width amplitude increased in ten equal steps
10 to reach the maximum considered crack width w_{max} (Fig. 5). This would be typical for mean
11 cycle counts of buildings subjected to the design earthquake in regions of moderate to high
12 seismicity. For further discussion see Wood¹³.

13 The maximum considered crack width was defined as $w_{max} = 0.8$ mm (0.03 in.), which
14 has been shown to be typical of characteristic crack widths occurring in concrete flexural
15 members at the onset of reinforcement yielding outside of plastic hinges¹⁷. For reference
16 purposes and to investigate the effect of maximum crack width on anchor performance, select
17 anchor products were also tested with $w_{max} = 0.5$ mm (0.02 in.), which is the specified crack
18 width for simulated seismic tests with cyclic loads according to ACI 355.2² and 355.4³. The
19 monotonic reference tests were carried out on anchors installed in wedge-split concrete slabs
20 with $w = w_{max}$. The averaged results allowed the determination of the mean monotonic
21 capacity $N_{u,mon,m}$ and its corresponding displacement $s(N_{u,mon,m})$.

22 The sustained tension load N_w applied during crack cycling is intended to represent the
23 load for which the tested anchor will be designed in applications. Because the seismic
24 capacity is unknown at the time of seismic qualification testing, N_w is taken as a fraction of its
25 mean monotonic capacity $N_{u,mon,m}$. In accordance with the safety concept underlying the

1 strength design of modern building codes such as the Eurocode 2¹⁸, the analyzed structural
2 element is shown to be safe if the design load N_{Ed} , i.e. the characteristic load N_{Ek} magnified
3 by the load safety factor γ_F , is less than the design strength N_{Rd} , i.e. the characteristic strength
4 N_{Rk} divided by the material safety factor γ_M ($N_{Ed} = N_{Ek} \cdot \gamma_F \leq N_{Rk} / \gamma_M = N_{Rd}$). A similar
5 equation can be written according ACI 318⁴, where factored loads are compared with
6 nominal strengths multiplied by the strength reduction factor ϕ . With the load safety factor
7 $\gamma_F = 1.0$ for load combinations governed by earthquake loads and the material safety factor
8 for concrete-related failure modes of $\gamma_M = 1.5$, this equation can be expressed as
9 $N_{Ed} \leq N_{Rk} / 1.5$. Assuming that the characteristic strength equals approximately 75 % of the
10 mean monotonic capacity ($N_{Rk} = 0.75 \cdot N_{u,mon,m}$)¹, the design strength can be taken as
11 $N_{Ed} \leq 0.75 \cdot N_{u,mon,m} / 1.5 = 0.5 \cdot N_{u,mon,m}$. Under earthquake conditions, however, the design
12 anchor load will not act permanently, but rather the load will vary as the structure and the
13 element that the anchor attaches respond dynamically. To account for this behavior, a factor
14 of 0.8 is applied the sustained tension load resulting in
15 $N_w = 0.8 \cdot N_{Ed} = 0.8 \cdot 0.5 \cdot N_{u,mon,m} = 0.4 \cdot N_{u,mon,m}$. The 0.8 factor is supported by
16 probabilistic investigations¹⁹ and has been confirmed by experimental studies²⁰. It noted that
17 it is acceptable to reduce the target load N_w to less than the above prescribed value during
18 testing to improve an anchor's seismic performance, however, the anchor will be assessed a
19 correspondingly reduced design capacity.

21 **Test setup and procedures**

22 After installation of the anchor, the strain-split slab was mounted in the testing rig by
23 connecting the high-strength tie rods to a fixed reaction frame on one side and to a 630 kN
24 (140 kip) horizontally-aligned servo-hydraulic actuator on the other side. Another 50 kN
25 (11 kip) vertically-aligned servo-hydraulic actuator was placed on supporting beams and

1 connected to the anchor. Mechanical anchors were tested under unconfined conditions with a
2 clear distance between the supporting beams of four times the effective embedment depth
3 (h_{ef}). Adhesive anchors were tested under confined conditions to ensure bond failure. For the
4 confined configuration, a smooth sheet of polytetrafluoroethylene (PTFE) and a steel plate
5 with a clearance hole equal to ≈ 2.0 times the drill hole diameter (d_0) were placed around the
6 anchor (Fig. 6a).

7 Load measurements were captured using load cells placed co-linear with the actuators.
8 A displacement transducer was connected to the top of the anchor using a pulley and magnet
9 and transducers were placed on either side of the anchor to measure crack width (Fig. 6b).
10 The measured crack width provided the input signal for control of the actuator force applied
11 to the concrete test member. A cyclic crack history was imposed by controlled ramps at
12 quasi-static rates of about 20 seconds per cycle (≈ 0.05 Hz). Although high loading rates
13 increase concrete and steel strength, anchor behavior at increased loading rates is complicated.
14 Importantly, the loading rates which would significantly affect anchor behavior are faster
15 than those anticipated under seismic loading, thus tests with low cycling frequencies are more
16 practical and yield conservative results compared to high cycling frequencies^{21,22}. Based on
17 previous research¹⁰, full crack closure was assumed to correspond to the concrete gross cross-
18 section area stressed to 12 % of the nominal concrete compressive strength, i.e. $0.12 \cdot f'_c$. The
19 target axial tension load of N_w was applied during crack cycling using a separate control
20 system from that used to load the concrete specimen. After completion of the crack cycles,
21 the anchor was unloaded and the concrete test member relaxed and the remaining
22 displacement after cycling (s_{cyc}) was determined (Fig. 2). To determine the residual axial load
23 capacity of the anchor, a tension test was then performed, while the 630 kN actuator opened
24 the crack load controlled to the specified maximum crack width of 0.5 mm or 0.8 mm
25 (0.02 in. or 0.03 in.) depending on the test series. This approach was observed to generate

1 crack conditions that are comparable to those created by the restoring forces of reinforcement
2 in the wedge-split concrete slabs used for the reference tests. As in the monotonic reference
3 tests, the anchor was loaded to failure in 1 minute to 3 minutes, resulting in the residual
4 capacity of the cyclic crack test $N_{u,cyc,m}$ and its corresponding displacement $s(N_{u,cyc,m})$. Anchor
5 load, anchor displacement, and crack width were measured and recorded at a sampling rate of
6 5 Hz.

8 **EXPERIMENTAL RESULTS AND DISCUSSION**

9 It is noted that the test conditions with respect to maximum crack width as well as the
10 maximum anchor load were more demanding than those for which the anchors had been
11 previously qualified. Thus, any adverse load-displacement behavior should not be considered
12 to disqualify the investigated anchors from the qualification guidelines in effect at the time.

14 **Anchor performance and displacement behavior**

15 The test program and a summary of key test results are provided in Table 2. The
16 subscripts u , mon , cyc and m stand for ultimate, monotonic, cyclic and mean. Figs. 7 and 8
17 show typical cyclic load-displacement curves and the corresponding monotonic mean curve
18 calculated as the average of the monotonic reference tests. All anchors that completed crack
19 cycling were tested to failure to determine their residual capacity. The observed anchor
20 failure modes included concrete breakout, pull-through, pullout and bond failure. Sufficient
21 steel strength and embedment depths precluded anchor steel failure.

22 All **load-displacement curves** demonstrate a characteristic load plateau representing
23 the crack cycling phase of the test, where constant anchor tension load was imposed and the
24 anchor displacement incrementally increases. It is noted that the initial loading branch of the
25 cyclic crack tests is generally steeper than that of the monotonic reference tests. The reason

1 for this is that the permanent load was applied at a crack width of $w_{max} / 10$ whereas the
2 monotonic reference tests were carried out with a crack width equal to w_{max} . The stiffness of
3 the load-displacement curves of concrete anchors increases with decreasing crack width¹. The
4 load-displacement curves from the cyclic crack tests with the undercut anchor UA1 showed
5 little cumulative anchor displacement during crack cycling (Fig. 7f). All undercut anchor
6 samples failed by concrete cone breakout when loaded to failure during monotonic tension
7 tests following the crack cycling. This suggests that undercut anchors are relatively
8 insensitive to crack cycling, even with large crack widths, if sufficient mechanical interlock is
9 provided to bridge the open crack. The behavior of expansion anchors, which transfer load by
10 friction, is different for the two tested expansion anchor types. While the sleeve-type
11 expansion anchor (EAs1) failed by concrete cone breakout (Figs. 7a and b), the bolt-type
12 expansion anchors (EAb1 and EAb2) experienced pull-through, with the anchor bolts pulling
13 through the relatively thin expansion elements (Figs. 7c to e). This failure mode shows dome-
14 shaped ascending and descending load-displacement curves with a displacement span
15 approximately equal to the height of the expansion element. The load-displacement behavior
16 and residual capacity is bounded by the monotonic curve. Screw anchors transfer load via
17 their threads cutting into the concrete forming multiple small, mechanical interlocks. During
18 loading, the concrete between the threads deteriorates and the anchor is ultimately pulled out
19 of its borehole. Despite the similarity of the load transfer mechanism of screw anchors and
20 cast-in deformed reinforcing bars, the displacement at peak load of the tested screw anchor
21 (SA1) was around 3 mm (0.12 in.) (Figs. 8a and b) and thus in general larger than that for
22 cast-in reinforcing bars of similar diameter, which is known to be generally between 1 mm
23 and 2 mm (0.04 in. and 0.08 in.). This may be attributed to the larger thread spacing of the
24 screw anchors if compared to the ribs of reinforcing bars. This trend corroborates similar
25 observations by Hoehler and Eligehausen¹⁰ in which screw anchors with large thread spacing

1
2
3 1 of 15 mm (0.59 in.) survived over 8 mm (0.31 in.) of displacement without shearing of the
4
5 2 concrete between the threads. The relationship between the interlock depth and the crack
6
7 3 width also plays an important role for screw anchors. If the crack opens more than the
8
9 4 interlock depth, the anchor will pull out of the concrete. Bonded anchors transfer tension
10
11 5 loads to concrete by adhesion and micro-interlock with the concrete along the entire
12
13 6 embedment depth. Confined test setups force bonded anchors to fail by bond failure. The
14
15 7 high-strength threaded rods of the tested bonded anchors (BA1, BA2 and BA3) were pulled
16
17 8 out partly with, partly without, the mortar. While the residual capacity after the cyclic crack
18
19 9 tests was significantly smaller than in monotonic tests (Figs. 8c to e), some bonded anchors
20
21 10 did not complete all crack cycles and could not be tested for residual capacity (Fig. 8f). An
22
23 11 additional advantage of stepwise-increasing crack amplitudes over constant or decrease
24
25 12 amplitudes is that they provide an indication of the maximum sustainable crack width for an
26
27 13 anchor even if all of the cycles are not successfully completed. This allows for faster test
28
29 14 iteration to obtain allowable anchor design capacities.

30
31
32
33
34 15 The dissimilar displacement behavior of the investigated anchor types can be observed
35
36 16 in the **displacement accumulated during crack cycling** s_{cyc} (Fig. 9a). This displacement
37
38 17 depends not only on the anchor response to the investigated crack cycling protocol, but also
39
40 18 on the level of the sustained load N_w , since larger loads lead to larger displacements. The
41
42 19 mechanical interlock of undercut anchors limits the displacements during cycling to less than
43
44 20 3 mm (0.12 in.), which is the displacement limit specified for non-seismic crack movement
45
46 21 tests according to ACI 355.2² and ACI 355.4³, as well as ETAG 001⁴ and below which a
47
48 22 connection is assumed to be rigid according to some building codes²¹. The tested expansion
49
50 23 anchors developed large displacements of up to 12 mm (0.48 in.) during crack cycling with a
51
52 24 follow-up expansion behavior as demonstrated by the residual load test. In contrast, the
53
54 25 displacement capacity of bonded anchors is smaller and sudden failure occurs once the
55
56
57
58
59
60

1
2
3 1 adhesion is destroyed ($s_{cyc} \rightarrow \infty$). While the tested screw anchor SA1 completed the crack
4
5 2 cycling with less than 3 mm (0.012 in.) of displacement, as discussed above, this is related to
6
7 3 the specific thread spacing and depth of the anchor.
8
9

10 4 For anchors completing crack cycling, the mean **residual ultimate load capacities**
11
12 5 $N_{u,cyc,m}$ were in general smaller than the corresponding capacities $N_{u,mon,m}$ of the reference
13
14 6 tests (Fig. 9b). The reduction in capacity is caused by the damaging of the concrete in the
15
16 7 vicinity of the anchor due to the repetitive compression and the anchor displacement toward
17
18 8 the concrete surface during crack cycling and resulting reduction of embedment depth. Only
19
20 9 for the investigated undercut and sleeve-type expansion anchors (UC1 and EAs1) were the
21
22 10 ratios of $N_{u,cyc,m} / N_{u,mon,m}$ larger than or close to 1.0. Despite the limited number of test
23
24 11 repeats, the scatter of the failure loads for these two anchor types was low with coefficients of
25
26 12 variation v less than 15 %, which is consistent with anchors failing in concrete-related failure
27
28 13 modes under non-seismic conditions¹. For the investigated screw anchor (SA1) as well as the
29
30 14 bonded anchors (BA1, BA2, BA3), the coefficients of variation of the residual load capacities
31
32 15 (where available) were considerably higher (above 20 %). No residual capacity is reported for
33
34 16 test series of bonded anchors where at least one tested anchor failed during crack cycling
35
36 17 ($N_{u,m} \rightarrow 0$). The coefficients of variation for the bolt-type expansion anchors in the residual
37
38 18 capacity tests varied between 4.9 % (EAb1) to 15.8 % (EAb2). The coefficient of variation of
39
40 19 the residual load capacity provides an indication of the robustness of the anchor under a
41
42 20 specific set of conditions; a smaller coefficient of variation is preferable.
43
44
45
46

47 21 The mean **anchor displacements** $s(N_{u,cyc})_m$ of the cyclic crack tests were always larger
48
49 22 than the corresponding displacements $s(N_{u,mon})_m$ of the reference tests (Fig. 9b), resulting in
50
51 23 ratios of $s(N_{u,cyc})_m / s(N_{u,mon})_m$ which are larger than 1.0. The displacements of the cyclic crack
52
53 24 tests ranged from less than 3 mm (0.12 in.) for the bonded anchor BA1 to more than 20 mm
54
55 25 (0.80 in.) for the bolt-type expansion anchor EAb1 and equaled approximately the
56
57
58
59
60

1
2
3 1 displacements of the monotonic reference tests $s(N_{u,cyc})_m$ plus the displacements accumulated
4
5 2 during cycling s_{cyc} .

6
7 3 As mentioned above, the peak residual load for anchors failing by concrete cone
8
9 4 breakout, i.e. undercut and sleeve-type expansion anchors (UA1 and EAs1), is greater than
10
11 5 the mean value in monotonic reference tests. This behavior was reported in previous
12
13 6 studies^{17,23} and is attributed to the compaction of the concrete during crack cycling at the
14
15 7 point of tension load transfer. Although excessive damage due to concrete compaction
16
17 8 decreases load capacity, limited compaction is presumed to have a beneficial effect on
18
19 9 residual strength. The curves of the residual load tests for the investigated bolt-type
20
21 10 expansion anchors (EAb1 and Eab2), failing by pull-through, and the screw anchor (SA1),
22
23 11 failing by pullout, are approximately bounded by the mean curve of the monotonic reference
24
25 12 tests. This agrees with previous findings¹⁰. New in this study are the results for adhesive
26
27 13 anchors. The residual load-displacement curves for the investigated bonded anchors (BA1,
28
29 14 BA2, BA3), failing by bond failure, do not reach the mean curve of their monotonic reference
30
31 15 tests. The tension load transfer mechanism for adhesive anchors in cracks, which relies on
32
33 16 micro-interlock once adhesion is lost, often results in a spontaneous failure during crack
34
35 17 cycling. This makes the **displacement capacity** of adhesive anchors during or after crack
36
37 18 cycling more difficult to predict than for mechanical anchors.

38
39 19 Because load is constant during crack cycling, it is also useful to visualize time-
40
41 20 histories to understand anchor behavior. Fig. 10 shows the anchor load and displacement as
42
43 21 well as the crack width as a function of time for a tested undercut anchor UA1. It is noted that
44
45 22 other investigated anchors showed a similar behavior. During crack cycling under sustained
46
47 23 anchor tension load, the anchor slips when the crack is opened, and is held in place when the
48
49 24 crack is closed. The amplitude of anchor displacement increment per cycle increases with
50
51 25 increasing crack width amplitude. The **energy dissipation** by the anchor during crack cycling

1 is negligible ($N_w \cdot s_{cyc}$) because the load-displacement curves do not exhibit hysteresis (refer to Fig 7. and Fig. 8)

2
3 The anchor products tested in 0.5 mm and 0.8 mm (0.02 in. and 0.03 in.) cracks (EAs1, EAb1, SA1 and BA1) demonstrated that the **crack width** in a monotonic test as well as the maximum crack width during cycling have a significant influence on the test results. Larger crack widths result in reduced anchor capacities²⁴. Furthermore, for a given anchor load, the incremental displacement during crack cycling increases with increasing crack width, resulting in a greater reduction of the residual capacity. For the tests presented in this paper, however, the permanent anchor loads applied during cyclic crack tests were defined as 0.4 times the mean failure load in monotonic reference tests which is lower for tests with $w_{max} = 0.8$ mm (0.03 in.) compared to tests with $w_{max} = 0.5$ mm (0.02 in.) cracks. For this reason, the reduction of residual capacity due to larger crack widths is counteracted by the increase due to lower sustained tension anchor loads (N_w). This may lead to larger ratios of $N_{u,cyc,m} / N_{u,mon,m}$ for the cyclic crack tests with $w_{max} = 0.8$ mm (0.03 in.) when compared with tests conducted with $w_{max} = 0.5$ mm (0.02 in.).

17 **Tests with increased number of crack cycles**

18 Some seismic events may impose larger crack widths and an increased number of deformation cycles. For this reason, some of the anchor products were also tested with a target maximum crack width of $w_{max} = 0.8$ mm (0.03 in.) and with additional crack cycles. To this end, the number of crack cycles in each step of the crack protocol developed by Wood¹⁵ were recalculated using a more stringent Rainflow cycle binning strategy, resulting in an additional 9 cycles across the crack width steps, thus an increase in number of crack cycle by about 30 %. Fig. 5 compares this crack protocol consisting of 41 cycles to the original protocol with 32 cycles. It is noted that while these protocol are similar to those found in

1
2
3 1 Wood's report¹⁴, they are not identical. The development of the protocol was an iterative
4
5 2 process with input from both the numerical and experimental studies.
6

7
8 3 Exploratory tests with the more severe cycle count were carried out on EAb1 and UC1
9
10 4 anchors installed in 0.8 mm (0.03 in.) cracks. Key results from these tests are presented in
11
12 5 Table 3. Fig. 11 shows load-displacement curve for EAb1 along with the corresponding test
13
14 6 conducted with original number of cycles for reference. The increased number of cycles
15
16 7 resulted in substantially increased anchor displacements, however, the reduction in
17
18 8 embedment depth was too small to significantly affect the residual capacities. This agrees
19
20 9 with previous findings for undercut anchors under simulated seismic crack cycling¹⁴. It is
21
22 10 noted that 7 out of the 9 additional cycles were added to the low amplitude cycles
23
24 11 ($w \leq 0.5 \cdot w_{max}$). The effect of increased number of crack cycles would be more pronounced if
25
26 12 more high amplitude cycles ($w > 0.5 \cdot w_{max}$) were added.
27
28
29
30
31
32
33

34 35 36 37 38 39 40 41 42 43 44 45 46 47 48 49 50 51 52 53 54 55 56 57 58 59 60

15 During earthquakes, structures undergo reversed cyclic deformation, which may cause
16 opening and complete closing of cracks in reinforced concrete structures. If post-installed
17 concrete anchors are located in these cracks, which is likely since anchors tend to attract
18 cracks, the anchor behavior may be significantly affected by the crack cycling. This paper
19 extends previous studies on the behavior of post-installed anchors during strong earthquakes
20 by providing comprehensive experimental results utilizing a newly-developed stepwise-
21 increasing crack cycling protocol. Five mechanical and three adhesive anchors that represent
22 most common post-installed concrete anchor types and failure modes were tested. Monotonic
23 tension tests with the anchors installed in 0.5 mm (0.02 in.) and 0.8 mm (0.03 in.) wide
24 cracks were first performed. Subsequently, 40 % of mean monotonic failure load was applied
25 as a sustained tension load on the anchors while the crack in which the anchor was installed

1 was cycled according to the new protocol. Zero crack width was assumed to correspond to a
2 compressive stress applied to the test specimen equal to 12 % of the concrete compressive
3 strength. Additional tests were performed in which the total number of crack cycles was
4 increased by 30 %.

5 All anchors exhibited increased displacements during crack cycling. The increase was
6 greater for larger maximum crack widths and a larger number of crack cycles. The tests
7 demonstrated that the investigated undercut anchor could survive crack cycling expected
8 during strong earthquakes. Moreover, the residual capacity of the undercut anchor was not
9 reduced relative to its monotonic capacity. Similar results were observed for the investigated
10 sleeve-type expansion anchor. The investigated bolt-type expansion anchors survived the
11 simulated seismic crack cycling, but exhibited a 15 % reduction in the residual capacity. The
12 investigated screw anchor and adhesive anchors showed significantly reduced performance
13 during crack cycling, which is believed to be due to the small thread spacing (screw anchor)
14 and micro-interlock (adhesive anchor) being damaged during the crack cycling. They may
15 show an acceptable behavior if the seismic design strength of the anchor in tension is
16 significantly reduced compared to the non-seismic design strength.

17 The tests described in this paper contributed to the development of the European
18 guideline ETAG 001 Annex E²⁵, which is valid for seismic loading and introduces new test
19 conditions and acceptance criteria, which are more demanding than the simulated seismic
20 tests currently in ACI 355.2² and ACI 355.4³.

21 22 **ACKNOWLEDGMENTS**

23 This research was funded by the Hilti Corporation. Opinions, conclusions, and
24 recommendations expressed in this paper are those of the authors and do not necessarily

1 reflect those of the sponsors or the authors' affiliations. The assistance of the staff at the
2 Anchor Laboratory of Stuttgart of University is greatly appreciated.

REFERENCES

1. Eligehausen R., Mallee R., Silva J., "Anchorage in concrete construction", Ernst & Sohn, Berlin, 2006.
2. ACI Committee 355, "Qualification of post-installed mechanical anchors in concrete (ACI 355.2-07) and commentary", American Concrete Institute, Farmington Hills, Michigan, 2007.
3. ACI Committee 355, "Acceptance criteria for qualification of post-installed adhesive anchors in concrete (ACI 355.4-11) and commentary", American Concrete Institute, Farmington Hills, Michigan, 2011.
4. ACI Committee 318, "Building code requirements for structural concrete (ACI 318-14) and commentary (ACI 318R-14)", American Concrete Institute, Farmington Hills, Michigan, 2014.
5. ETAG 001, "Guideline for European technical approval of metal anchors for use in concrete, Parts 1 – 6", European Organization of Technical Approvals (EOTA), Brussels. 1997.
6. Rehm G., Lehmann R., "Untersuchungen mit Metallspreizdübeln in der gerissenen Zugzone von Stahlbetonbauteilen (Investigations with metal expansion anchors in cracked reinforced concrete)", Fraunhofer Society Research Report V. 1015, 1982 (in German).
7. Lotze D., Faoro M., "Rißbreitenentwicklung und Dübelverschiebung bei veränderlicher Bauteilbelastung (Width development and fastener displacement under varying building component loads)", Report No. 1/28-88/3, Institut für Werkstoffe im Bauwesen, Universität Stuttgart, 1988 (in German).

- 1
2
3 1 8. Eligehausen R., Asmus J., „Zuverlässigkeitsprüfungen an Dübeln in Liniennissen
4 (Reliability tests on fasteners in line cracks)“, Report No. 1/49A-91/1A, Institut für
5
6 2
7 3 Werkstoffe im Bauwesen, Universität Stuttgart, 1991 (in German).
8
9 4 9. DIBt KKW Leitfaden, „Leitfaden für Dübelbefestigungen in Kernkraftwerken und anderen
10 5 kerntechnischen Anlagen (Guideline for fastenings in nuclear power plants and other nuclear
11 6 technical facilities)“, Deutsches Institut für Bautechnik (DIBt), Berlin, 2010 (in German).
12
13 7 10. Hoehler M., Eligehausen R., „Behavior and testing of anchors in simulated seismic
14 8 cracks“, ACI Structural Journal, V. 105, No. 3, May-June 2008, pp. 348-357.
15
16 9 11. EN 1992-1-1. Eurocode 2: Design of concrete structures – Part 1-1: General rules, and
17 10 rules for buildings”, European Committee for Standardization (CEN); EN 1992:2005.
18
19 11 12. EN 1998-1, “Eurocode 8: Design of structures for earthquake resistance – Part 1: General
20 12 rules, seismic actions and rules for buildings”, European Committee for Standardization
21 13 (CEN); EN 1998-1:2004.
22
23 14 13. Wood R., Hutchinson T., “Crack protocols for anchored components and systems”, ACI
24 15 Structural Journal, V. 110, No. 3, May-June 2013, pp. 391-401.
25
26 16 14. Wood R., Hutchinson T., Hoehler M., “Cyclic load and crack protocols for anchored
27 17 nonstructural components and systems”, Structural Systems Research Project (SSRP)
28 18 2009/12, University of California, San Diego, 2010.
29
30 19 15. Mahrenholtz P., “Experimental performance and recommendations for qualification of
31 20 post-installed anchors for seismic applications”, Dissertation, University of Stuttgart, 2012.
32
33 21 16. Mahrenholtz P., Eligehausen R., Hutchinson T., Hoehler, M., “Behavior of anchors tested
34 22 by stepwise increasing cyclic load protocols in tension and shear”, ACI Structural Journal
35 23 (accepted for publication).
36
37 24 17. Hoehler M., “Behavior and testing of fastenings to concrete for use in seismic
38 25 applications”, Dissertation, University of Stuttgart, 2006.
39
40
41
42
43
44
45
46
47
48
49
50
51
52
53
54
55
56
57
58
59
60

- 1
2
3 1 18. EN 1992, “Eurocode 2: Design of concrete structures”, European Committee for
4
5 2 Standardization (CEN); EN 1992:2004 +AC:2010.
6
7 3 19. Sharma A., Mahrenholtz C., Eligehausen R., Reddy G., Vaze K., Ghosh A., “Evaluation
8
9 4 of load on anchor for concrete structures corresponding to maximum crack width – A
10
11 5 probabilistic approach”, International Journal of Earth Sciences and Engineering, V. 3, No. 4,
12
13 6 pp. 798-811, 2010.
14
15 7 20. Mahrenholtz P., Hutchinson T., Eligehausen R., “Shake table tests on suspended
16
17 8 nonstructural components anchored in cyclically cracked concrete”, ASCE Journal of
18
19 9 Structural Engineering, V. 140, No. 11, November 2014.
20
21 10 21. Mahrenholtz C., Eligehausen R., “Dynamic performance of concrete undercut anchors for
22
23 11 Nuclear Power Plants”, Nuclear Engineering and Design, V. 265, 2013, pp. 1091-1100.
24
25 12 22. Hoehler, M., Mahrenholtz, P., Eligehausen, R., “Behavior of anchors in concrete at
26
27 13 seismic-relevant loading rates.” ACI Structural Journal, 108(2), 2011, pp. 238-247.
28
29 14 23. Furche J., “Zum Trag- und Verschiebungsverhalten von Kopfbolzen bei zentrischem Zug
30
31 15 (Load-bearing and displacement behavior of headed bolts under centric tension load)”,
32
33 16 Dissertation, University of Stuttgart, 1994.
34
35 17 24. Eligehausen R., Balogh T., “Behavior of fasteners loaded in tension in cracked reinforced
36
37 18 concrete. ACI Structural Journal, Vol. 92, No. 3, May-June 1995, pp. 365-379.
38
39 19 25. ETAG 001 Annex E, “Guideline for European Technical Approval of metal anchors for
40
41 20 use in concrete - Annex E: Assessment of metal anchors under seismic actions”, 2013.
42
43
44
45
46
47
48
49
50
51
52
53
54
55
56
57
58
59
60

LIST OF NOTATIONS

- 1
2
3 1
4
5 2
6
7 3
8
9
10 4 d_0 = Borehole diameter
11
12 5 f'_c = Concrete compression strength
13
14 6 h_{ef} = Effective embedment
15
16 7 $s(N)$ = Axial displacement
17
18 8 s_{cyc} = Residual displacement after load cycling
19
20 9 v = Coefficient of variation
21
22
23 10 w = Crack width
24
25 11 w_{max} = Target maximum crack width
26
27 12 N_w = Permanent axial load
28
29 13 $N_{u,m}$ = Mean ultimate tension load
30
31
32 14 N_{Rk} = Characteristic resistance
33
34 15 N_{Ek} = Characteristic load
35
36 16 γ_F = Load safety factor
37
38 17 γ_M = Material safety factor
39
40
41 18
42
43
44
45
46
47
48
49
50
51
52
53
54
55
56
57
58
59
60

TABLES AND FIGURES

List of Tables:

Table 1 – Investigated anchors.

Table 2 – Tests conditions and key test results of monotonic reference tests and crack cycling tests (values reported as average of all test repeats).

Table 3 – Tests conditions and key test results of cyclic crack tests with increased number of cycles (values reported as average of all test repeats).

List of Figures:

Fig. 1 – Concrete anchor loaded in tension and subjected to crack cycling.

Fig. 2 – Sample load-displacement diagram for crack movement test (cyclic and residual capacity test) and corresponding mean curve of monotonic reference tests according to ACI 355.

Fig. 3 – Tested anchor types with indicated transfer mechanism for tension load (located in opened crack): a) Undercut anchor (UC); b) Screw anchor (SA); c) Expansion anchor – sleeve-type (EAs); d) Expansion anchor – bolt-type (EAb); e) Bonded anchor (BA).

Fig. 4 – Strain-split concrete slab: a) Top view; b) Side view (units in mm (in.)).

Fig. 5 – Cyclic crack protocol (increased number of crack cycles in grey).

Fig. 6 – Test setup: a) Strain-split concrete slab (picture shows testing of an adhesive anchor with confined setup); b) Close-up to anchor (picture shows testing of a mechanical anchor with unconfined setup).

Fig. 7 – a) to f) Typical load-displacement curves of cyclic crack tests on undercut anchors and expansion anchors and corresponding mean curve of monotonic reference tests.

1
2
3 1 **Fig. 8 – a) to f)** Typical load-displacement curves of cyclic crack tests on screw and bonded
4 anchors and corresponding mean curve of monotonic reference tests.
5
6

7 3 **Fig. 9 –** Load and displacement behavior: a) Sustained tension load N_w versus displacement
8 during cycling s_{cyc} ; b) Ratios of capacities and corresponding displacements of cyclic crack
9 tests and monotonic reference tests.
10
11

12 6 **Fig. 10 –** Anchor load and displacement as well as crack width as a function of time
13
14 (example: undercut anchor with $w_{max} = 0.8$ mm (0.03 in.)).
15
16

17 8 **Fig. 11 –** Typical load-displacement curves of cyclic crack tests on expansion anchors – bolt-
18 type with different numbers of crack cycles as well as corresponding mean curve of
19
20
21
22
23 10 monotonic reference tests.
24
25

26 11
27
28
29
30
31
32
33
34
35
36
37
38
39
40
41
42
43
44
45
46
47
48
49
50
51
52
53
54
55
56
57
58
59
60

1
2
3
4
5
6
7
8
9
10
11
12
13
14
15
16
17
18
19
20
21
22
23
24
25
26
27
28
29
30
31
32
33
34
35
36
37
38
39
40
41
42
43
44
45
46
47
48
49
50
51
52
53
54
55
56
57
58
59
60

1

2

Table 1 – Investigated anchors.

Anchor designation	Anchor type	Nominal size	Steel element diameter, mm (in.)	Embedment depth h_{ef} , mm (in.)
UA1	Undercut	M10	10 (0.39)	90 (3.54)
SA1	Screw	Ø16	16 (0.63)	105 (4.13)
EAs1	Expansion, sleeve-type	M10	10 (0.39)	80 (3.15)
EAb1	Expansion, bolt-type	1/2 ^a	12.3 (0.5)	83 (3.25)
EAb2		1/2 ^a	12.3 (0.5)	86 (3.375)
BA1	Bonded epoxy-type	M12 ^b	12 (0.47)	96 (3.78)
BA2		M12 ^b	12 (0.47)	96 (3.78)
BA3	Bonded methacrylate-type	M12 ^b	12 (0.47)	96 (3.78)

3
4
5

^a UA: Undercut Anchor; SA: Screw anchor; EAs: Expansion anchor – sleeve-type; EAb: Expansion anchor – bolt-type; BA: Bonded anchor
^b Threaded rod with $f_y = 900$ MPa (130 ksi) and $f_u = 1000$ MPa (145 ksi)

Peer Review Only

Table 2 – Tests conditions and key test results of monotonic reference tests and crack cycling tests (values reported as average of all test repeats).

Anchor designation ^a	Target crack width w_{max} , mm	Load type ^b	Number of tests	Failure mode ^c	Sustained load N_w , kN	$N_{u,m}$, kN	$v^d(N_{u,m})$, %	$N_{u,cyc,m} / N_{u,mon,m}$	s_{cyc} , mm	$s(N_{u,m})$, mm	$v^d(s(N_{u,m}))$, %	$s(N_{u,cyc,m}) / s(N_{u,mon,m})$
UA1	0.8	mon	3	C	13.7	34.2	5.7	1.25	1.39	1.64	11.8	3.87
		cyc	3	C		42.6	8.5			6.35	17.6	
EAs1	0.5	mon	3	C	15.6	38.9	15.3	0.97	2.71	6.54	62.6	1.49
		cyc	3	C		37.9	7.8			9.76	23.5	
	0.8	mon	3	C	11.0	27.5	7.6	1.09	8.07	6.12	61.7	2.66
		cyc	3	C		29.9	8.2			16.28	11.4	
EAb1	0.5	mon	3	Pt	10.1	25.2	6.6	0.94	7.30	7.94	13.0	1.96
		cyc	3	Pt		23.8	13.9			15.57	17.1	
	0.8	mon	3	Pt	8.7	21.8	7.3	0.85	12.15	10.98	10.1	1.85
		cyc	3	Pt		18.5	4.9			20.31	25.4	
EAb2	0.8	mon	3	Pt	6.7	16.3	3.2	0.84	9.24	10.61	16.3	1.61
		cyc	3	Pt		13.6	15.8			17.03	25.7	
SA1	0.5	mon	3	Po	14.4	34.3	4.7	0.57	1.97	2.69	35.4	1.49
		cyc	3	Po		19.5	4.1			4.01	9.7	
	0.8	mon	3	Po	7.7	19.2	33.0	0.88	1.49	3.07	9.2	1.18
		cyc	3	Po		17.0	24.8			3.63	11.4	
BA1	0.5	mon	3	B	31.3	78.2	8.1	→ 0 ^e	→ ∞ ^e	1.21	29.5	→ ∞ ^e
		cyc	2	B ^e		→ 0 ^e	- ^e			→ ∞ ^e	- ^e	
	0.8	mon	3	B	25.0	62.6	10.3	→ 0 ^e	→ ∞ ^e	1.67	32.5	→ ∞ ^e
		cyc	2	B ^e		→ 0 ^e	- ^e			→ ∞ ^e	- ^e	
BA2	0.8	mon	3	B	17.5	41.4	14.2	0.68	0.92	0.97	24.3	3.06
		cyc	2	B		27.8	32.6			2.98	5.5	
BA3	0.8	mon	3	B	12.4	29.4	8.0	→ 0 ^e	→ ∞ ^e	1.14	13.9	→ ∞ ^e
		cyc	2	B ^e		→ 0 ^e	- ^e			→ ∞ ^e	- ^e	

^a UA: Undercut anchor; EAs: Expansion anchor – sleeve-type; EAb: Expansion anchor – bolt-type; BA: Bonded anchor

^b mon = monotonic; cyc = cyclic

^c Failure mode: C = Concrete breakout, Pt = pull-through, Po = Pullout, B = Bond failure

^d Coefficient of variation for one standard deviation

^e Pullout failure of all or some test repeats before completion of crack cycles

Note: Refer to Fig. 2 for explanation of variables; 1 mm = 0.0394 in.; 1 kN = 224.81 lbf.

4
5
6
7
8
9
10

1
2
3
4
5
6
7
8
9
10
11
12
13
14
15
16
17
18
19
20
21
22
23
24
25
26
27
28
29
30
31
32
33
34
35
36
37
38
39
40
41
42
43
44
45
46
47
48
49
50
51
52
53
54
55
56
57
58
59
60

1
2
3

Table 3 – Tests conditions and key test results of cyclic crack tests with increased number of cycles (values reported as average of all test repeats).

Anchor designation ^a	Target crack width w_{max} , mm	Load type ^b	Number of tests	Failure mode ^c	Sustained load N_w , kN	$N_{u,m}$, kN	$v^d(N_{u,m})$, %	$N_{u,cyc,m} / N_{u,mon,m}$	s_{cyc} , mm	$s(N_u)_m$, mm	$v^d(s(N_u)_m)$, %	$s(N_{u,cyc})_m / s(N_{u,mon})_m$
UA1	0.8	cyc	3	C	18.2	45.2	7.0	1.32	4.94	12.61	28.9	7.69
EAb1	0.8	cyc	3	Pt	8.7	19.5	24.2	0.89	14.23	19.97	21.6	1.82

4
5
6

^{a-d} Refer to Table 2
Note: Refer to Fig. 2 for explanation of variables; 1 mm = 0.0394 in.; 1 kN = 224.81 lbf.



1
2
3
4
5
6
7
8
9
10
11
12
13
14
15
16
17
18
19
20
21
22
23
24
25
26
27
28
29
30
31
32
33
34
35
36
37
38
39
40
41
42
43
44
45
46
47
48
49
50
51
52
53
54
55
56
57
58
59
60

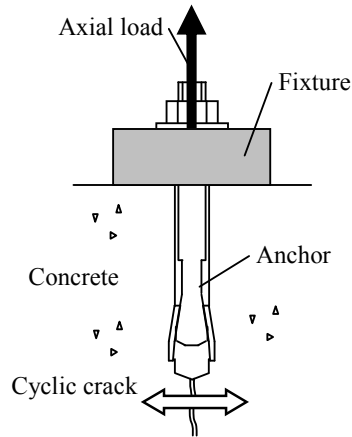


Fig. 1 – Concrete anchor loaded in tension and subjected to crack cycling.

For Peer Review Only

1
 2
 3 1
 4
 5 2
 6 3
 7 4
 8 5
 9 6
 10 7
 11 8
 12 9
 13 10
 14 11
 15 12
 16 13
 17 14
 18 15
 19 16
 20 17
 21 18
 22 19
 23 20
 24 21
 25 22
 26 23
 27
 28
 29
 30
 31
 32
 33
 34
 35
 36
 37
 38
 39
 40
 41
 42
 43
 44
 45
 46
 47
 48
 49
 50
 51
 52
 53
 54
 55
 56
 57
 58
 59
 60

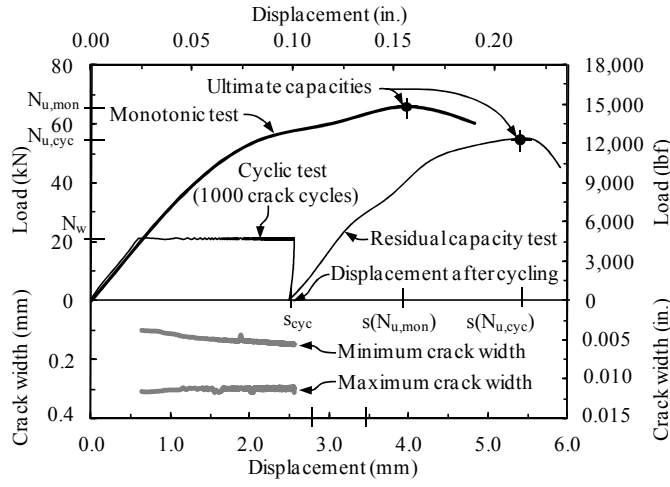


Fig. 2 – Sample load-displacement diagram for crack movement test (cyclic and residual capacity test) and corresponding mean curve of monotonic reference curve according to ACI 355.

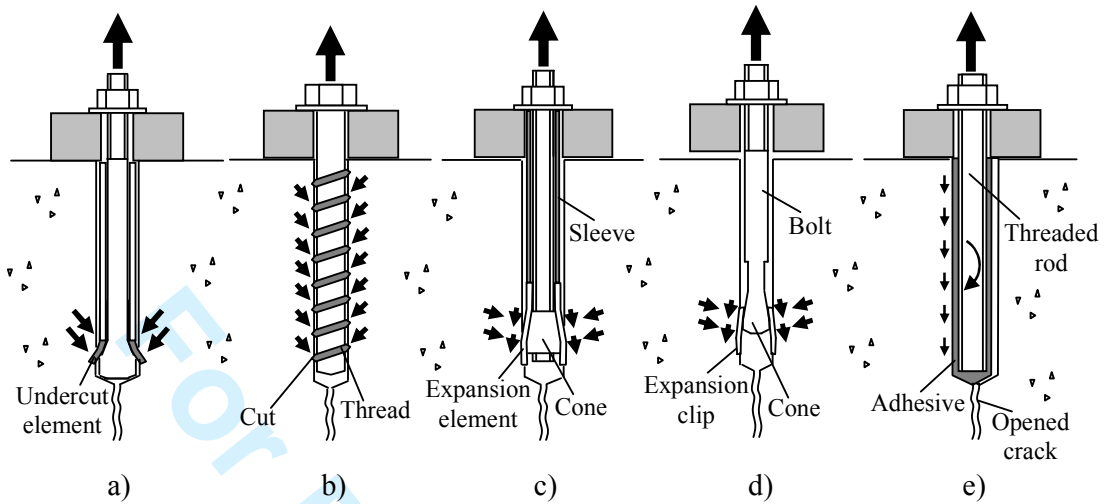


Fig. 3 – Tested anchor types with indicated transfer mechanism for tension load (located in opened crack): a) Undercut anchor (UC); b) Screw anchor (SA); c) Expansion anchor – sleeve-type (EAs); d) Expansion anchor – bolt-type (EAb); e) Bonded anchor (BA).

1
2
3
4
5
6
7
8
9
10
11
12
13
14
15
16
17
18
19
20
21
22
23
24
25
26
27
28
29
30
31
32
33
34
35
36
37
38
39
40
41
42
43
44
45
46
47
48
49
50
51
52
53
54
55
56
57
58
59
60

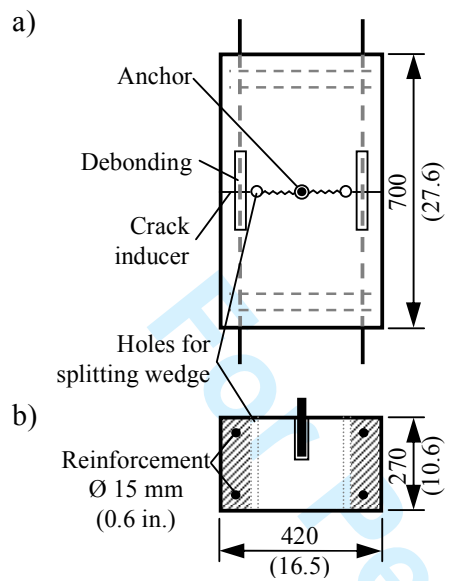


Fig. 4 – Strain-split concrete slab: a) Top view; b) Side view (units in mm (in.)).

1
2
3
4
5
6
7
8
9
10
11
12
13
14
15
16
17
18
19
20
21
22
23
24
25
26
27
28
29
30
31
32
33
34
35
36
37
38
39
40
41
42
43
44
45
46
47
48
49
50
51
52
53
54
55
56
57
58
59
60

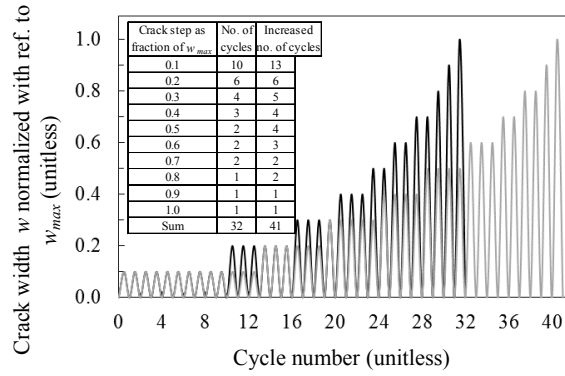


Fig. 5 – Cyclic crack protocol (increased number of crack cycles in grey).

1
2
3
4
5
6
7
8
9
10
11
12
13
14
15
16
17
18
19
20
21
22
23
24
25
26
27
28
29
30
31
32
33
34
35
36
37
38
39
40
41
42
43
44
45
46
47
48
49
50
51
52
53
54
55
56
57
58
59
60

1
2
3
4
5
6
7
8
9
10
11
12
13
14 a)
15
16
17
18
19
20
21
22
23
24
25
26
27
28 b)
29
30
31

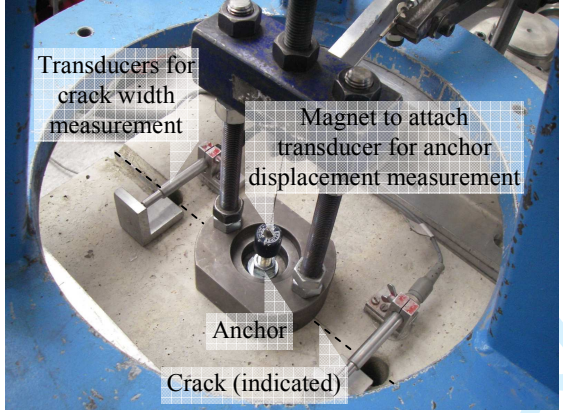
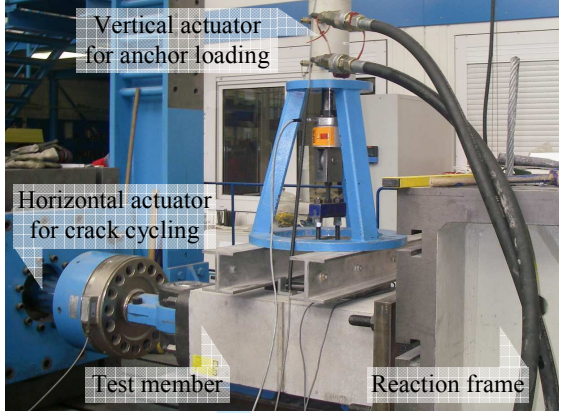
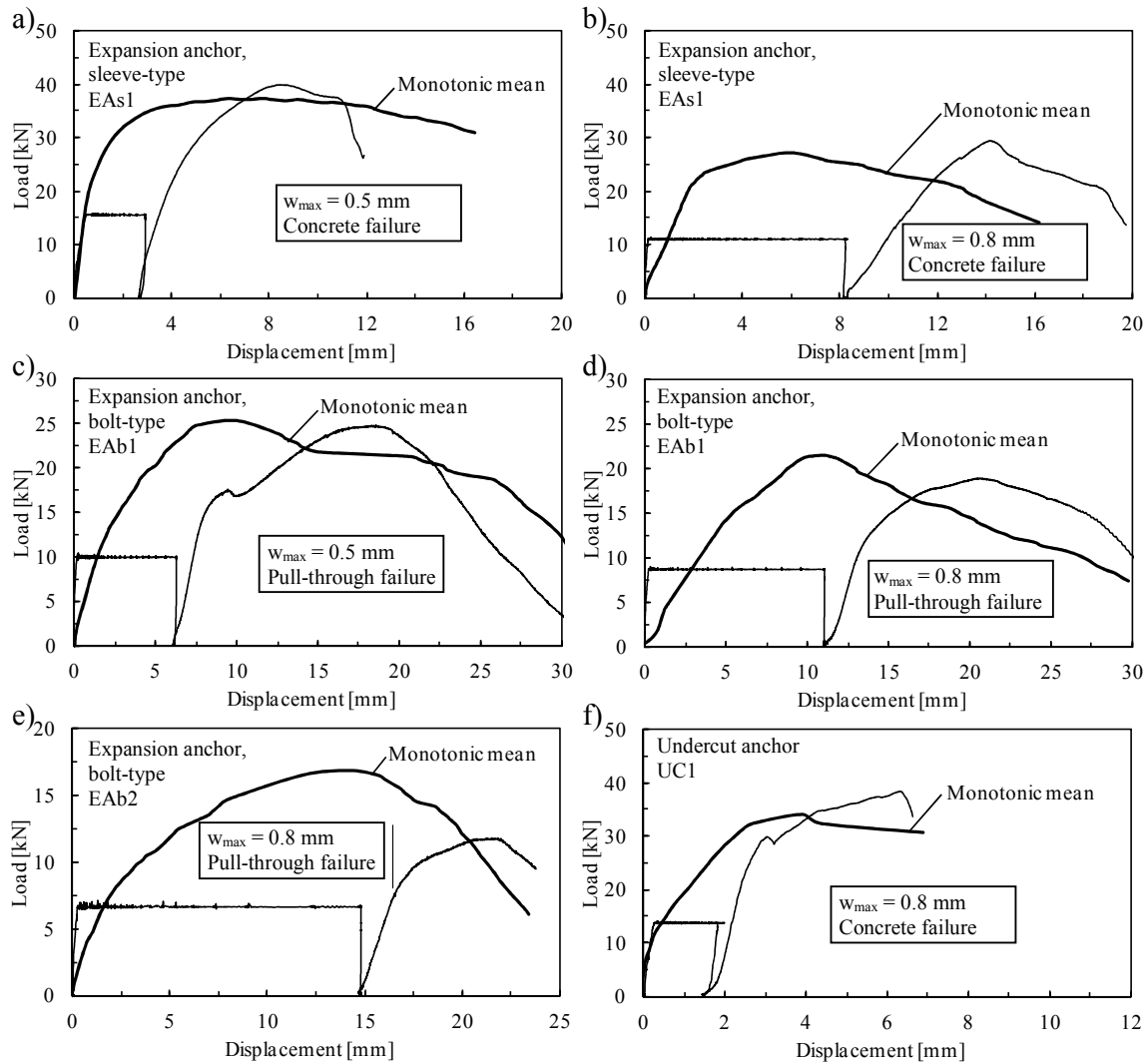


Fig. 6 – Test setup: a) Strain-split concrete slab with horizontal and vertical actuators; b) Close-up of anchor and instrumentation.

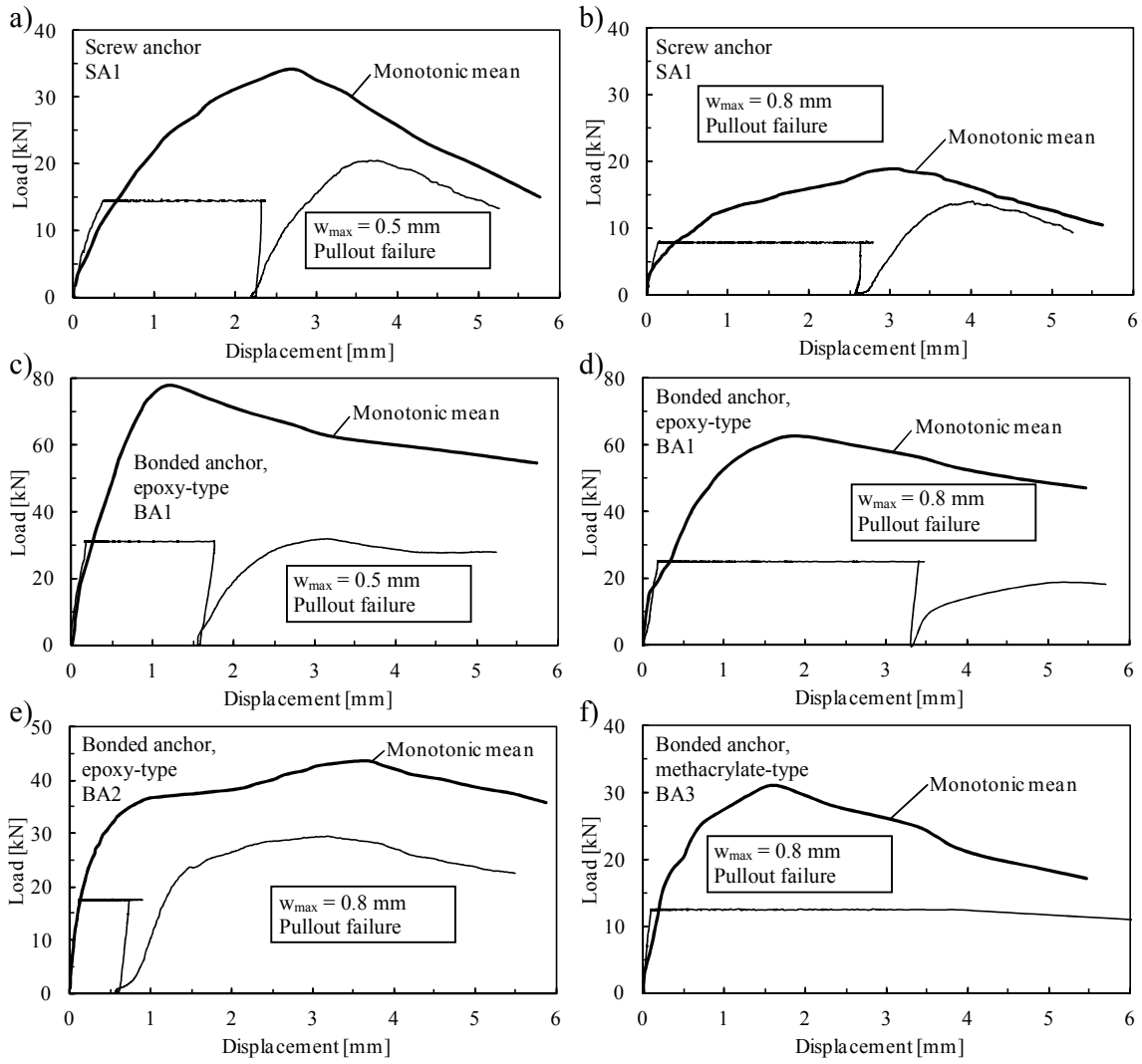
1
2
3
4
5
6
7
8
9
10
11
12
13
14
15
16
17
18
19
20
21
22
23
24
25
26
27
28
29
30
31
32
33
34
35
36
37
38
39
40
41
42
43
44
45
46
47
48
49
50
51
52
53
54
55
56
57
58
59
60



Note: 1 mm = 0.0394 in.; 1 kN = 224.81 lbf.

Fig. 7 – a) to f) Typical load-displacement curves of cyclic crack tests on undercut anchors and expansion anchors and corresponding mean curve of monotonic reference tests.

1
2
3
4
5
6
7
8
9
10
11
12
13
14
15
16
17
18
19
20
21
22
23
24
25
26
27
28
29
30
31
32
33
34
35
36
37
38
39
40
41
42
43
44
45
46
47
48
49
50
51
52
53
54
55
56
57
58
59
60



Note: 1 mm = 0.0394 in.; 1 kN = 224.81 lbf.

Fig. 8 – a) to f) Typical load-displacement curves of cyclic crack tests on screw anchors and bonded anchors and corresponding mean curve of monotonic reference tests.

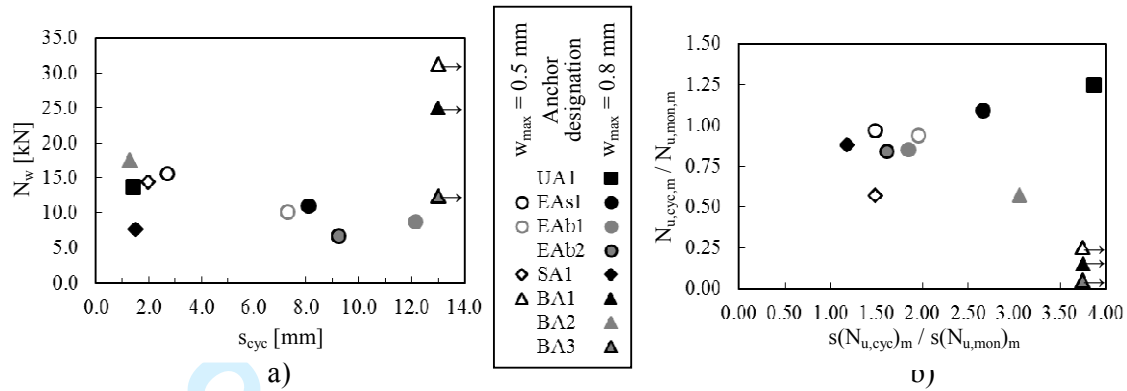


Fig. 9 – Load and displacement behavior: a) Sustained tension load N_w versus displacement during cycling s_{eye} ; b) Ratios of capacities and corresponding displacements of cyclic crack tests and monotonic reference tests.

1
2
3
4
5
6
7
8
9
10
11
12
13
14
15
16
17
18
19
20
21
22
23
24
25
26
27
28
29
30
31
32
33
34
35
36
37
38
39
40
41
42
43
44
45
46
47
48
49
50
51
52
53
54
55
56
57
58
59
60

1
2
3
4
5
6
7
8
9
10
11
12
13
14
15
16
17
18
19
20
21
22
23
24
25
26
27
28
29
30
31
32
33
34
35
36
37
38
39
40
41
42
43
44
45
46
47
48
49
50
51
52
53
54
55
56
57
58
59
60

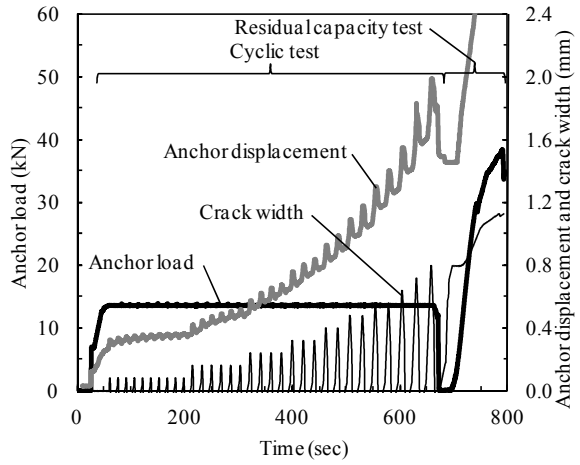
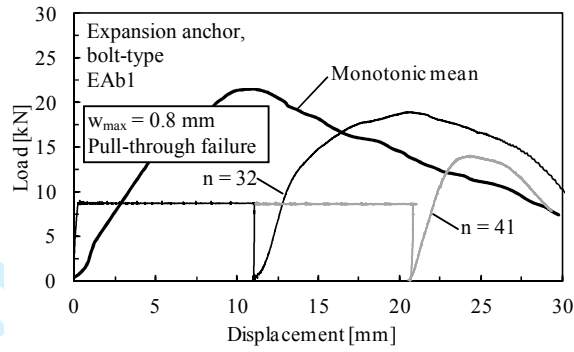


Fig. 10 – Anchor load and displacement as well as crack width as a function of time (example: undercut anchor with $w_{max} = 0.8$ mm (0.03 in.)).



Note: 1 mm = 0.0394 in.; 1 kN = 224.81 lbf.

Fig. 11 – Typical load-displacement curves of cyclic crack tests on expansion anchors – bolt-type with different numbers of crack cycles as well as corresponding mean curve of monotonic reference tests.